# Linking soil biology and chemistry using bacterial isolate exometabolite profiles

Tami L. Swenson[1], Ulas Karaoz[2], Joel M. Swenson[3], Benjamin P. Bowen[1,4], Trent Northen[1,4]*

[1]Environmental Genomics and Systems Biology Division, Lawrence Berkeley National Laboratory, 1 Cyclotron Rd, Berkeley, California 94720, USA.

[2]Climate and Ecosystems Sciences Division, Lawrence Berkeley National Laboratory, 1 Cyclotron Rd, Berkeley, California 94720, USA.

[3]Biological Systems and Engineering Division, Lawrence Berkeley National Laboratory, 1 Cyclotron Rd, Berkeley, California 94720, USA.

[4]DOE Joint Genome Institute, 2800 Mitchell Dr., Walnut Creek, California 94598, USA.

*Corresponding author: E-mail: TRNorthen@lbl.gov*

## ABSTRACT

Sequencing provides a window into microbial community structure and metabolic potential; however, linking these data to exogenous metabolites that microorganisms process and produce (the exometabolome) remains challenging. Previously, we observed strong exometabolite niche partitioning among bacterial isolates from biological soil crust (biocrust). Here we examine native biocrust to determine if these patterns are reproduced in the environment. Overall, most soil metabolites displayed the expected relationship (positive or negative correlation) with four dominant bacteria following a wetting event and across biocrust developmental stages. For metabolites that were previously found to be consumed by an isolate, 78% were negatively correlated with the abundance of *in situ* isolate phylotypes whereas for released metabolites, 73% were positively correlated. Our results demonstrate that metabolite profiling, sequencing and exometabolomics can be successfully integrated to functionally link metagenomes and microbial community structure with environmental chemistry.

In soils, which harbor the largest terrestrial pool of organic carbon[1], organic matter is largely processed by complex microbial communities. The impact of climate change on these communities and their activities is uncertain[2]. Given the importance of these systems, vast amounts of sequencing data have been and continue to be collected. While metagenomic sequencing provides important insights into community structure and metabolic potential, if unconstrained, such data are often open to multiple interpretations. New approaches are needed to help link the now readily available sequencing data to *in situ* metabolism in order to better understand the dynamic reciprocity between carbon cycling and microbial community structure.

Soil organic matter (SOM) content and moisture have long been recognized as important factors controlling soil microbial community structure and carbon cycling[3,4]. For example, microbial community diversity and richness are positively correlated with soil organics across diverse ecosystems including polar soils[5], agricultural soils[6] and arid soils[7]. Similarly, soil wetting events are well-known to dramatically alter community structure[8] including establishing cascades of microbial abundances[9]. Arid lands account for over 40% of Earth's terrestrial surface[10] and are especially sensitive to SOM and moisture content. It is predicted that the aridity of drylands will increase, reducing SOM and microbial community diversity, and that this will impact ecosystem productivity[7,11]. This strong coupling between soil moisture, SOM and community structure is especially important in the arid land topsoil microbial communities known as biological soil crusts (biocrusts), which cover a large fraction of arid regions and are critical in nutrient cycling[12]. Biocrusts exist in a dormant desiccated state and only become metabolically

active during infrequent rainfall events[13] and like other soils, organic matter plays a vital role in retaining moisture and increasing microbial diversity[14].

The mechanisms linking SOM composition and microbial community structure are poorly understood. It is now thought that the organic matter that is cycled by soil microbes is a complex mixture of microbial metabolites[15,16] that can be characterized in detail using soil metabolomics[17,18]. The composition of these exometabolites has a large impact on community structure, and in turn, these microbes impact the metabolite pool. For example, in some cases, resource competition can reduce diversity through competitive exclusion, whereas cross-feeding can increase diversity. On the other hand, rich sources of SOM may promote diversity through niche divergence[19] and exometabolite niche partitioning[20].

Exometabolomics enables direct examination of how microbes transform the small molecule metabolites within their environment, providing new insights into resource competition and cross-feeding[21]. For this approach, microbes (typically isolates) are cultured in an environmentally-relevant mixture of metabolites and then spent media is profiled to determine the uptake and release of metabolites. Recently, exometabolomics was used to study resource partitioning among sympatric biocrust isolates using complex media[20]. This revealed a high degree of substrate specialization where 13-26% of the detected metabolites were consumed by individual isolates. As organisms from diverse taxa continue to be cultivated and examined, this approach holds substantial potential to provide valuable phenotypic information that can link community structure to SOM composition.

Here we explored the dynamics and relationships between biocrust microbes and metabolites. We then determined the extent to which isolate exometabolite patterns are conserved *in situ* (within the intact soil community). Microbe-metabolite changes were driven by wetting dry biocrusts obtained along an ecological successional gradient (Figure 1A). Four successional stages of biocrust were used, ranging from early/ young (labeled as 'level A') to late/ mature (labeled as 'level D') (Supplementary Figure 1). We then compared our current results with previous laboratory-derived knowledge of substrate preferences for four dominant organisms by relating the abundance of these bacteria to soil metabolites measured in the intact biocrust system (Figure 1B). While the comparison of a microbe in isolation and in an environmental system is complex, the general assumption is that as a particular microbe grows and increases in abundance in a community, consumed metabolites will decrease and display a negative-correlation relationship. Conversely, metabolites that are known to be released by a microbe are predicted to concurrently increase and display a positive-correlation relationship with growth (Figure 1B). Liquid chromatography-mass spectrometry (LC/MS) soil metabolomics was used to characterize the dynamic composition of the biocrust soil water and shotgun metagenomic sequencing was used to measure single copy gene markers of the dominant taxa. To the best of our knowledge, this is the first study using isolate exometabolomics to link microbial community structure to soil chemistry.

## RESULTS

### *Cycling of metabolites and microbes across wetting and successional stages*

The metabolic activity caused by wetting was monitored at various time points ranging from immediate (3 min) to long-term (49.5 h) across the four biocrust successional stages. Biocrust soil water was analyzed by LC/MS, resulting in the identification of 85 metabolites using authentic chemical standards (Figure 2 and Supplementary Table 1). All metabolites displayed cycling by changing at least two-fold (between minimum and maximum peak areas) across both wetting and successional stages (Figure 2). Wetting duration had a stronger impact on metabolite dynamics compared to changes in successional stages (Supplementary Figure 2). Hierarchical clustering of metabolite patterns revealed three distinct clusters (Figure 2). The first cluster (cluster 1, Figure 2) consisted of most (5 out of 7) of the detected fatty acids (palmitate, myristate, stearate, laurate, decanoate), which were most abundant at the first time point (3 min) for all successional stages, and gradually decreased with time. The largest cluster (cluster 2, Figure 2) was enriched with the majority of amino acids and nucleobases, which peaked in abundance at the early to early-mid time points. Within this cluster, the earliest metabolites included polar amino acids (glutamine, glutamate, asparagine, 4-oxoproline, aspartate and lysine) and the nucleobases uridine, guanosine and cytidine. The final cluster (cluster 3 in Figure 2) contained metabolites most abundant at late time points and in more mature biocrust (*e.g.* salicylate, panthothenate, nicotinate, xanthine, creatinine).

Microbial community structure was determined using shotgun metagenomics with a genome-centric analysis pipeline. The relative abundances of environmental genomes

were determined via read-mapping to a universal single-copy phylogenetic marker gene, *rplO* (ribosomal protein L15)[22]. This approach has proven useful in several reports for examination of community structure via shotgun sequencing that often results in poor 16S ribosomal RNA gene assemblies[23-25]. Based on *rplO* genes, 466 distinct organisms were identified in the biocrust across all conditions (Supplementary Table 2). As observed for biocrust metabolites, community structure was primarily driven by time since wetting. At the phylum level, the most drastic change was a shift from a cyanobacteria-dominated community at early time points (17-28% at 3 min to 1-3% by 49.5 h) to a Firmicutes-dominated community by 49.5 h (4-5% at 3 min to 19-39% by 49.5 h) (Supplementary Figure 3). Other dominant phyla included Proteobacteria and Actinobacteria, which appeared to be indifferent to wetting (*i.e.* their relative abundance was more evenly-distributed across wetting) (Supplementary Figure 3).

In order to use previous exometabolomic studies to link soil microbe-metabolite abundances in biocrust, *rplO* gene sequences of the profiled biocrust bacterial isolates[20] were compared to all *rplO* genes obtained from biocrust. With this approach, we identified four relatively abundant isolate-related phylotypes in the biocrust that were selected for further analyses and exometabolomics comparisons: *Microcoleus* spp. (a filamentous Cyanobacterium and primary producer), two Firmicutes (referred to here as *Anoxybacillus* sp. and *Bacillus* sp.) and *Blastococcus* sp. (an actinobacterium) (Table 1, Supplementary Figure 4). *Microcoleus* spp. is known to be a pioneer species responsible for initial soil stabilization and biocrust formation[26] and in our study was the most dominant in early wetup biocrust, accounting for 10-25% of the entire microbial community at 3 min across all successional stages (Supplementary Figure 5). The two

149 Firmicutes, *Anoxybacillus* sp. and *Bacillus* sp., are likely to be physically-associated with
150 *Microcoleus* filaments[20] and their relative abundance increased during wetting. The
151 most abundant of these, *Anoxybacillus sp.*, was a mid-wetup responder and peaked at
152 9 h for successional levels A, B and D (16-24% of the community) and at 18 h for
153 successional level C (24% of the community) (Supplementary Figure 5). *Bacillus* sp.
154 reached its peak abundance at later time points, accounting for up to 3% of the
155 community by 42 h in successional level C (Supplementary Figure 5), noting that by the
156 later time points the community was less dominated by any one particular organism
157 (Supplementary Figure 5). Finally, *Blastococcus* sp. abundance was found to be
158 relatively resistant to wetting and was somewhat evenly distributed across all conditions
159 (0.1-2% of the community) (Supplementary Figure 5).
160
161 ***Linking microbe-metabolite abundances based on isolate exometabolomics***
162 ***profiling***
163 To determine how isolate substrate preferences impacted *in situ* exometabolite
164 composition, we evaluated microbe-metabolite correlations, focusing on metabolites
165 known to be released or consumed by the related isolates of *Microcoleus* spp.,
166 *Anoxybacillus* sp., *Bacillus* sp. and *Blastococcus* sp. The expectation was that released
167 metabolites would be positively correlated with the relative bacterial abundance while
168 consumed metabolites would be negatively correlated (Figure 1B) across both wetting
169 and successional stage. To link previous isolate exometabolomics data with the current
170 biocrust exometabolome dataset (Figure 2), we determined the degree of correlation
171 between the metabolites that were previously found to be consumed and released by

172 biocrust isolates[20] and the four relatively-abundant bacteria of interest found in the
173 biocrust (*Microcoleus* spp., *Anoxybacillus* sp., *Bacillus* sp. and *Blastococcus* sp). Of the
174 85 metabolites identified in the biocrust soil water, 32 matched the isolate
175 exometabolome dataset (Supplementary Table 3).

176 To assess the directionality (positive versus negative correlations) of predicted
177 soil microbe-metabolite relationships, we performed Spearman's rank correlation
178 analyses. We then used an exact binomial test to evaluate the possibility that the
179 correct directionality could occur by chance (Supplementary Table 4). Strikingly, of the
180 71 microbe-metabolite relationships evaluated (Supplementary Figure 6), 76% had the
181 predicted directionality and would be very unlikely to occur by chance (two-tailed p-
182 value < $1 \times 10^{-5}$; Supplementary Table 4).

183 We next used our data to hypothesize a dynamic exometabolomic web of
184 microbes, largely reflecting the release of metabolites by the primary producer
185 (*Microcoleus* spp.*)* followed by consumption by the two heterotrophs that displayed a
186 large degree of cycling across wetting (*Anoxybacillus* sp. and *Bacillus* sp.) (Figure 3).
187 *Blastococcus* sp. is not shown in Figure 3 since this organism did not drastically change
188 across time and to simplify visualization of the network. Of the large set of metabolites
189 that were most highly-released by *M. vaginatus* PCC 9802[20], 20 of these were detected
190 in the biocrust soil water and most (65%) were positively correlated with *Microcoleus*
191 spp. (Figure 3 and Supplementary Figure 6) across wetting and successional stages.
192 While *Microcoleus* spp. was most abundant immediately following wetting, most of
193 these metabolites (80%) reached their highest level during the first three time points (3

194 min, 9 h or 18 h) just after the *Microcoleus* spp. spike, suggesting release by
195 *Microcoleus* spp. followed by increasing consumption by heterotrophs.
196 Consistent with a heterotrophic lifestyle, metabolites were primarily negatively
197 correlated with the abundances of *Anoxybacillus* sp., *Bacillus* sp. and *Blastococcus* sp.
198 Of the metabolites that were consumed by the *Anoxybacillus* sp.- related isolate, D1B51
199 (Table 1)[20], 12 were detected in the current biocrust soil water samples and reached
200 their highest level early-on (at either 3 min, 9 or 18 h), decreasing just after the peak in
201 *Anoxybacillus* sp. Nine of these metabolites were negatively correlated with
202 *Anoxybacillus* sp., consistent with metabolite consumption, and all four D1B51-released
203 metabolites were positively correlated with *Anoxybacillus* sp. (Figure 3 and
204 Supplementary Figure 6). As for the less dominant organisms, the late-wetup
205 responder, *Bacillus* sp., was negatively correlated with all 10 metabolites that were
206 consumed by the related isolate (L2B47) and positively correlated with 4 out of 5
207 isolate-released metabolites (Figure 3 and Supplementary Figure 6). Furthermore,
208 *Blastoccocus* sp., was negatively correlated with 13 out of the 15 metabolites that were
209 consumed by the related isolate (L1B44), while a single isolate-released metabolite was
210 positively correlated (tryptophan; Supplementary Figure 6). Finally, the closest biocrust
211 phylotypes of the three remaining exometabolomic-profiled isolates (L1B56, D1B2 and
212 D1B45) accounted for 0.1% or less of the microbial community in our metagenomes
213 and thus, not surprisingly, did not display exometabolite-based microbe-metabolite
214 relationships (data not shown).
215
216 **Transcriptomics support the link between soil microbes and metabolites**

217 Transcriptomics has the potential to test if gene expression is consistent with the
218 predicted substrate utilization and release. As an initial proof of concept, we further
219 analyzed data obtained from a previous study that evaluated *M. vaginatus* gene
220 expression following wetup and drydown in biocrusts obtained from the same field
221 site[27]. We found that pathways involved in the biosynthesis of amino acids (KEGG
222 pathways 'biosynthesis of amino acids', 'phenylalanine, tyrosine and tryptophan
223 biosynthesis' and 'valine, leucine and isoleucine biosynthesis') all increased
224 dramatically during early wet-up (Supplementary Figure 6, Supplementary Table 5). In
225 contrast, pathways involved in the degradation of these same metabolites were
226 relatively constant ('phenylalanine metabolism') or only slightly increased ('tryptophan
227 metabolism' and 'valine, leucine and isoleucine biosynthesis') following wet-up
228 (Supplementary Figure 7) consistent with the early-increase of most amino acids in
229 biocrust soil water in the present study and the release of these metabolites by *M.*
230 *vaginatus* PCC 9802[20].
231
232 **DISCUSSION**
233 Sequencing has the potential to link exometabolite composition to specific
234 microbes based on genome annotations. However, based on these data alone, relating
235 metabolic potential to activity is challenging. Despite this, sequencing and other
236 approaches have started to shed light on the impact individual organisms[28], microbial
237 genes[29] and enzymatic activities[30] have on the chemistry within their environment. Here,
238 we evaluated exometabolite profiles of individual bacteria for linking soil metabolites to

239 bacteria in biocrust, a critical ecosystem that lends itself to studies of community
240 responses to soil wetting.

241 We found that a wetting event set in motion an immediate cascade of microbial
242 activities marked by a drastic shift in community structure. The dominance of
243 Cyanobacteria during early time points is consistent with previous reports[31] as is the
244 subsequent Firmicutes-bloom[9,32]. The Firmicutes phylum consists mostly of gram-
245 positive, spore-forming bacteria with rapid generation times, enabling them to 'bloom'
246 upon soil wetting[33,34]. The observed switch from a Cyanobacteria-dominated community
247 to a Firmicutes-dominated community (mostly *Anoxybacillus* sp. in this study) agrees
248 with our observations of metabolite release by the dominant photoautotroph
249 (*Microcoleus* spp.)[20] followed by consumption and growth of diverse heterotrophs (*e.g.*
250 Firmicutes), possibly including symbiotic nitrogen-fixers[35]. While we did not observe
251 evidence of fixed nitrogen transfer into Cyanobacteria, this process may occur during
252 dry-down, when nitrogen-rich nutrients may be released upon the mother cell lysis stage
253 of sporulation[36].

254 It has been suggested that copiotrophic organisms (*e.g.* many Firmicutes) are
255 superior competitors for a limited number of compounds whereas oligotrophs (*e.g.* many
256 Actinobacteria) support a more stable population by using a wider range of substrates[37].
257 Our previous exometabolomics work is consistent with this view and showed that the
258 two Firmicutes isolates depleted the narrowest range of substrates (10%) whereas the
259 two Actinobacteria used almost twice as many[20]. Here we find that unlike the boom-bust
260 cycle of Fimicutes, the Actinobacteria phylum (such as *Blastococcus* sp.) may be more
261 resistant to wetting. This provides limited evidence that utilization of diverse substrates,

consistent with oligotrophy, may enable slow but continuous growth under conditions with highly dynamic exometabolite pools.

The community dynamics that were caused by biocrust wetting resulted in strong microbe-metabolite relationships that were conserved from one successional stage to another for the four bacteria of interest (*Microcoleus* spp., *Anoxybacillus* sp., *Bacillus* sp. and *Blastococcus* sp.) (Supplementary Figure 8). This supports the notion that the water-soluble SOM in these biocrusts, to a large degree, originates from and is controlled by microbes[15] and the composition of this pool may be predictable if a change in microbial community structure is anticipated. This finding has particular significance for biocrusts, since changes in temperature and rainfall are expected to shift microbial community structure[38,39]. As a result, these alterations are expected to impact SOM cycling especially if there is loss of taxa responsible for utilization or production of specific SOM components.

Next, we explored the connection between the observed microbe-metabolite relationships in biocrust and culture-based exometabolite profiles. Overall, we found that isolate exometabolomic patterns were conserved in the intact biocrust soil microbial community. The expected directionality (positive or negative microbe-metabolite correlations) (solid arrows in Figure 3) was significantly higher than predicted by chance, indicating a linkage between laboratory observations and *in situ* soil activities. While most metabolites displayed the expected patterns, some biocrust soil water metabolites (*i.e.* uracil, N6-acetyl-lysine, hypoxanthine and xanthine) were inconsistent with *M. vaginatus* PCC 9802 exometabolite profiles. However, these were also released by and positively correlated with *Bacillus* sp. Deconvoluting this may be possible using

dynamic utilization models[40,41] to account for the relative contributions of the two organisms. Ultimately, this same approach could be used to account for rare community members that may also have an impact on the exometabolite pool or may alter the metabolism of other microbes[42,43]. Although outside of the scope of the current work, we anticipate that these substrate-genome linkages could be further tested and refined by using other approaches. Stable isotope probing coupled with labeled DNA sequencing[35,44] and integrated NanoSIMS and FISH imaging[45,46] may be used to examine the spatial localization of microbes and their activities.

We next used the biocrust microbe-metabolite relationships to postulate a dynamic exometabolomics web describing the wetting response of three dominant bacteria in the biocrust (Figure 3). This network displays the release of many metabolites, especially amino acids, by *Microcoleus* spp. followed by consumption by the two heterotrophic Firmicutes. This suggests unique organismal roles in the biocrust foodweb including the preferential consumption of aromatic amino acids (tryptophan and phenylalanine) by *Anoxybacillus* sp. and branched-chain amino acids (leucine and isoleucine) by both Firmicutes. Interestingly, we also observe that these Firmicutes release nucleobases (uracil, hypoxanthine and xanthine), consistent with our earlier reports of heterotrophs releasing these compounds[47]. This may reflect a nitrogen-scavenging mechanism by consuming N-containing substrates (cytosine, adenine, guanine and histidine), producing uracil, hypoxanthine, xanthine and urocanate as byproducts. Knowledge of these functional linkages between metabolites and microbes has the potential to help understand and predict nutrient cycling in terrestrial microbial ecosystems[48] analogously to the many organisms that have been linked to specific

308 transformations within marine ecosystems. For example Cyanobacteria release and
309 reuptake organic carbon[49], a variety of uncultured taxa utilize dissolved proteins[44] and
310 SAR11 bacteria assimilate amino acids and dimethylsulfoniopropionate[50].
311 We attribute much of the success of this study to the suitability of the biocrust
312 ecosystem. One such advantage is that biocrust soil in this study is primarily quartz
313 sand, facilitating metabolite analysis compared to many other soils which are typically
314 rich in clays and other strongly-sorptive mineral surfaces[51]. Accurately representing the
315 competition between microbes and mineral surfaces would require additional studies
316 examining mineral-metabolite sorption dynamics[52,53]. Another relatively simplifying
317 factor is that the biocrust community, unlike many other soils, is dominated by a few
318 bacteria, greatly enabling accurate correlations between taxa and metabolites.
319 Furthermore, there is a general lack of consensus of isolate-to-community comparisons
320 and what constitutes a valid comparison especially with the use of ribosomal protein
321 genes as phylogenetic markers. Exometabolite-profiled isolates and their related
322 biocrust phylotypes ranged between 86.3-92.0% identical in their *rplO* sequence (Table
323 1), likely placing them in the same genus, and with more certainty, the same family.
324 Despite the low taxonomic resolution, the observed functional similarity, agrees with
325 reports suggesting that metabolic traits are largely conserved at the phylum level[54]. We
326 anticipate that in order to accurately predict microbe-metabolite relationships for more
327 diverse communities and complex environments, a large number of relevant taxa would
328 need to be subjected to exometabolite profiling. Accounting for switching between
329 metabolic states will require profiling under diverse environmental conditions. For
330 example, the discrepancy between metabolites that were released by *M. vaginatus* PCC

9802[20], but were not correlated with *Microcoleus* spp. abundance in the present study may be due to different metabolic processes occurring during the day (photosynthesis) versus night (respiration) (Diel cycle)[27,55]. Thus, modeling approaches will be required to account for metabolic state switching among other processes. One exciting possibility of expanded exometabolomic datasets, is that knowledge of uptake and release of metabolites can be used as boundary constraints for flux-balance analysis[56] and trait-based models[57] providing a genome-scale approach for linking soil metabolites with metagenomic data. For example, OptCom[58], a multi-level and multi-objective flux balance analysis framework to understand metabolism within microbial communities, which currently primarily relies on genomic information, could be used in conjunction with exometabolomic data.

In conclusion, this study shows that isolate exometabolite patterns are conserved within an intact biocrust community, relating community structure and metabolite composition. We expect that exometabolomic characterization of additional taxa and determination of mineral-metabolite sorption dynamics, under a range of environmentally relevant conditions (e.g. day/night cycles), integrated with modeling approaches will further enhance the predictive power of these relationships. These studies may help pave the way for interpretation and use of metagenomic and metatranscriptomic approaches for linking soil chemistry to soil microbiomes to define exometabolite webs of microbes in complex ecosystems.

## MATERIALS AND METHODS:

### *Materials*

LC/MS-grade water and LC/MS-grade methanol (CAS 67-56-1) were from Honeywell Burdick & Jackson (Morristown, NJ). LC/MS-grade acetonitrile (CAS 75-05-8) and ammonium acetate (CAS 631-61-8) were from Sigma-Aldrich (St. Louis, MO). LC/MS internal standards included MOPS (CAS 1132-61-2), HEPES (CAS 7365-45-9), 3,6-dihydroxy-4-methylpyridazine (CAS 5754-18-7), 4-(3,3-dimethyl-ureido)benzoic acid (CAS 91880-51-2), $d_5$-benzoic acid (CAS 1079-02-3) and 9-anthracenecarboxylic acid (CAS 723-62-6) from Sigma-Aldrich.

### *Sample collection*

Petri dishes (6 $cm^2$ x 1 cm depth) were used to core biocrust samples from the Green Butte Site near Canyonlands National Park (38°42'54.1"N, 109°41'27.0"W, Moab, UT, USA). Samples were collected along an apparent maturity gradient of Cyanobacteria-dominated biocrusts ranging from light, young (level A) to darker, more mature (level D) (Supplementary Figure 1). Samples were air-dried in the field and brought back to the laboratory where they were maintained in a dark desiccation chamber.

### *Biocrust wetting*

Biocrust (0.5 g) was transferred to each well within 12-well plates. Sterile LC/MS-grade water (1 mL) was added to each sample and placed under a 12 h light (~300 µmol photons/$m^2$s)/ 12 h dark cycle. Microcosms were completely enclosed by

aluminum foil to prevent infiltration by outside light sources. At each time point (3 min, 9 h, 18 h, 42 h and 49.5 h), biocrust and soil water were removed and placed in 2 mL Eppendorf tubes and 500 µL of additional water was used to rinse out the wells and added to the sample. Tubes were centrifuged at 5000 x *g* for 5 min and supernatant (biocrust soil water) was pipetted and placed in new 2 mL tubes. Remaining biocrust was stored at -80°C until nucleic acid extraction was performed. There were five replicates, five time points and four successional stages of crust resulting in 100 total samples.

***Metabolite extraction and LC/MS analysis***

Biocrust soil water samples (1.5 mL) were lyophilized and resuspended in methanol (200 µL) containing internal standards (2-10 µg/mL) and filtered through 96-well Millipore filter plates (0.2 µm PVDF) by centrifuging at 1500 x *g* for 2 min. Samples were analyzed using normal-phase LC/MS with a ZIC-pHILIC column (150 mm × 2.1 mm, 3.5 µm 200 Å, Merck Sequant, Darmstadt, Germany) using an Agilent 1290 series UHPLC (Agilent Technologies, Santa Clara, California, USA). Chromatographic separation was achieved using two mobile phases, 5 mM ammonium acetate in water (A) and 90% acetonitrile w/ 5 mM ammonium acetate (B) at a flow rate of 0.25 mL/min with the following gradient: 100% B for 1.5 min, linear decrease to 50% B by 25 min, held until 29.9 min then returned to initial conditions by 30 min with a total runtime of 40 min. Column temperature was maintained at 40°C. For MS, negative mode data were acquired on an Agilent 6550 quadrupole time-of-flight mass spectrometer and positive mode data were acquired on a Thermo QExactive (Thermo Fisher Scientific, Waltham,

399 MA). Fragmentation spectra (MS/MS) were acquired for some metabolites using
400 collision energies of 10-40 eV.

401 Metabolomics data were analyzed using Metabolite Atlas[59] in conjunction with
402 the Python programming language. Internal standards were assessed from each
403 sample to ensure peak area and retention times were consistent from sample-to-
404 sample. Quality control mixtures were included at the beginning, end and throughout the
405 runs to ensure proper instrument performance (*m/z* accuracy and retention time and
406 peak area stability). Sample QC failed for some replicates including all 9 h wetup level D
407 samples and were not included for further analyses. Metabolite identifications were
408 based on two orthogonal data relative to authentic standards and/or the Metlin
409 database[60,61] and are provided in Supplementary Table 1. Putative identifications were
410 assigned in the cases where these criteria were not met and are indicated by
411 parentheses in figures. To explore the degree of variation in biocrust metabolite profiles
412 across wetting and successional stages, biocrust samples were PCA-ordinated based
413 on their metabolite profiles.

414

415 ***DNA extraction, sequencing and microbial annotation***

416 DNA was extracted from biocrust (0.25 g) using the MoBio Powersoil DNA
417 isolation kit (MoBio Laboratories, Inc, Carlsbad, CA) resulting in 100 uL of eluted DNA.
418 Library preparation and sequencing were done at the QB3 facility at the University of
419 California, Berkeley using Illumina HiSeq4000 (see supplementary methods for details
420 on metagenome analysis). In recent studies[23-25], ribosomal protein genes have been
421 used as phylogenetic markers as an alternative to the more classical 16S ribosomal

RNA gene. Ribosomal protein genes exist as single copies in almost all genomes, assemble well from metagenome datasets, are well-conserved and have produced higher resolution phylogenetic trees[23]. Given these advantages, the 50S ribosomal protein L15 (*rplO*) gene was well-represented in our metagenomes and was therefore used as a phylogenetic marker to examine the relative abundance of individual organisms within the microbial community across wetting and successional stages. The *rplO* genes from the genomes of the seven exometabolite profiled biocrust bacterial isolates[20] were compared to all the *rplO* genes recovered from biocrust. Those with the highest percent similarity were considered the "closest relatives" to the isolates and are reported in Table 1.

***Microbe-metabolite correlations and statistics***

Correlations were used to identify microbe-metabolite relationships across both wetting and successional stages. Spearman's rank (*rho*) correlation coefficients for every pairwise (microbe-metabolite) relationship and p-values (unadjusted and FDR-adjusted) were calculated using the cor() stats function in R. A Spearman's *rho* value greater than or equal to 0.5 was considered "highly correlated" and less than or equal to -0.5 was considered "highly negatively correlated". To test if the overall observed directionality (positive versus negative correlations) was due to chance rather than as would be predicted based on exometabolomics (release versus consumption), the exact binomial test was conducted using R (binom.test) with a total of 71 "trials" or observed microbe-metabolite interactions (Supplemental table 4).

### *Exometabolomics comparison and analysis*

Of the 85 metabolites detected in biocrust soil water, 32 were previously analyzed for consumption and release by biocrust isolates[20]. For continued analyses of those data here, fold-change was calculated by dividing the average peak area of each metabolite in (isolate) inoculated spent media by the non-inoculated control spent media (raw data can be found in the Supplemental Table in Baran et al, 2015). A metabolite was considered consumed if the fold-change was 0.5 or less and released metabolites had a fold-change of 2 or greater.

### *Microcoleus gene expression analysis*

*Microcoleus* genes from Supplementary Table S6 from Rajeev et al (2013) were categorized into KEGG pathways (for genes containing KEGG ID numbers). Analyses focused on pathways that are primarily anabolic or catabolic for metabolites that were released by *Microcoleus* PCC 9802. The average fold-change (relative to dry biocrusts) and standard errors were calculated for all genes belonging to pathways of interest.

## ACKNOWLEDGEMENTS

This work was funded by the Office of Science Early Career Research Program, Office of Biological and Environmental Research, of the U. S. Department of Energy under contract number DE-AC02-05CH11231. DNA was sequenced using the Vincent J. Coates Genomics Sequencing Laboratory at UC Berkeley, supported by NIH S10 OD018174 Instrumentation Grant. We thank Rebecca Lau for technical assistance in biocrust sample collection and experimentation.

468

469 **AUTHOR CONTRIBUTIONS**

470 T.L.S. and T.R.N. conceived the study, designed the experiments and wrote the
471 manuscript. T.L.S. performed the experiments. T.L.S. and B.P.B. analyzed the
472 metabolomics data. U.K. analyzed the metagenomics data. T.L.S. and J.M.S.
473 conducted correlation and statistical analyses. All co-authors commented on the design
474 of experiments, data analysis and draft manuscripts.

475

476

## FIGURES AND TABLES

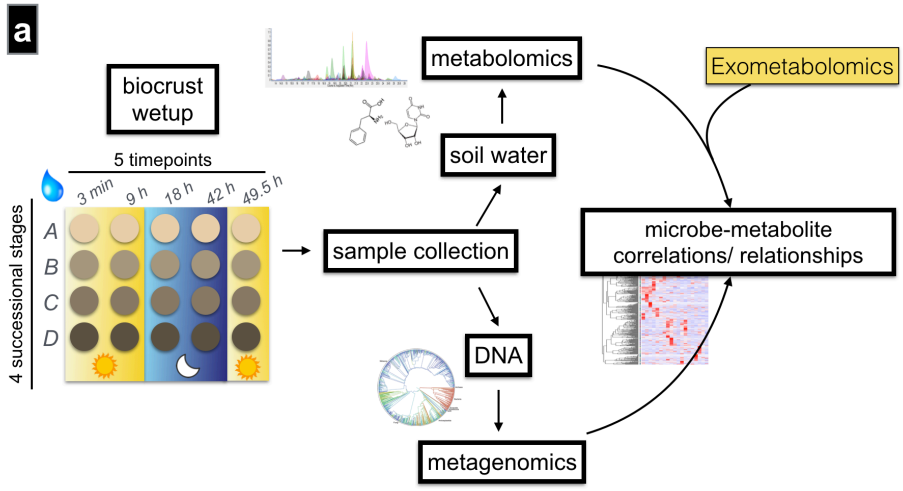


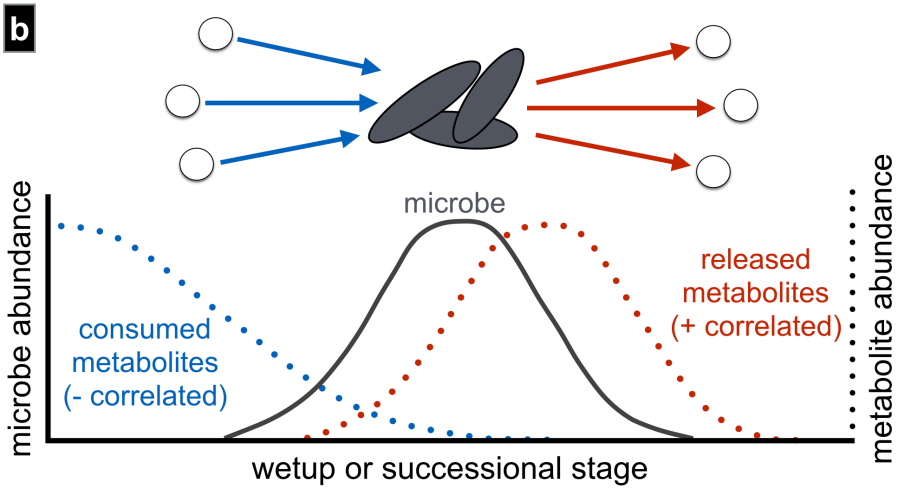


**Figure 1.**
**A. Biocrust wetup metabolomics and metagenomics experimental setup and analysis.** To study microbe-metabolite relationships *in situ*, biocrusts from four successional stages were wetup and sampled at five time points. Biocrust soil water was removed and analyzed by liquid chromatography/ mass spectrometry and biocrust DNA was extracted for sequencing. Metagenome-estimated genome and metabolite abundances were analyzed through rank correlations to determine microbe-metabolite relationships and compared to the expected relationships based on isolate exometabolomic studies.
**B. Exometabolomics-based *in situ* microbe-metabolite relationship prediction.** The hypothesis is that isolate exometabolomics can be used to predict microbe-metabolite patterns *in situ* based on microbial abundance: Across wetting and successional stages, microbes change in abundance and negatively correlate with metabolites that they consume and positively correlate with metabolites that they release (metabolites are indicated by dotted lines).

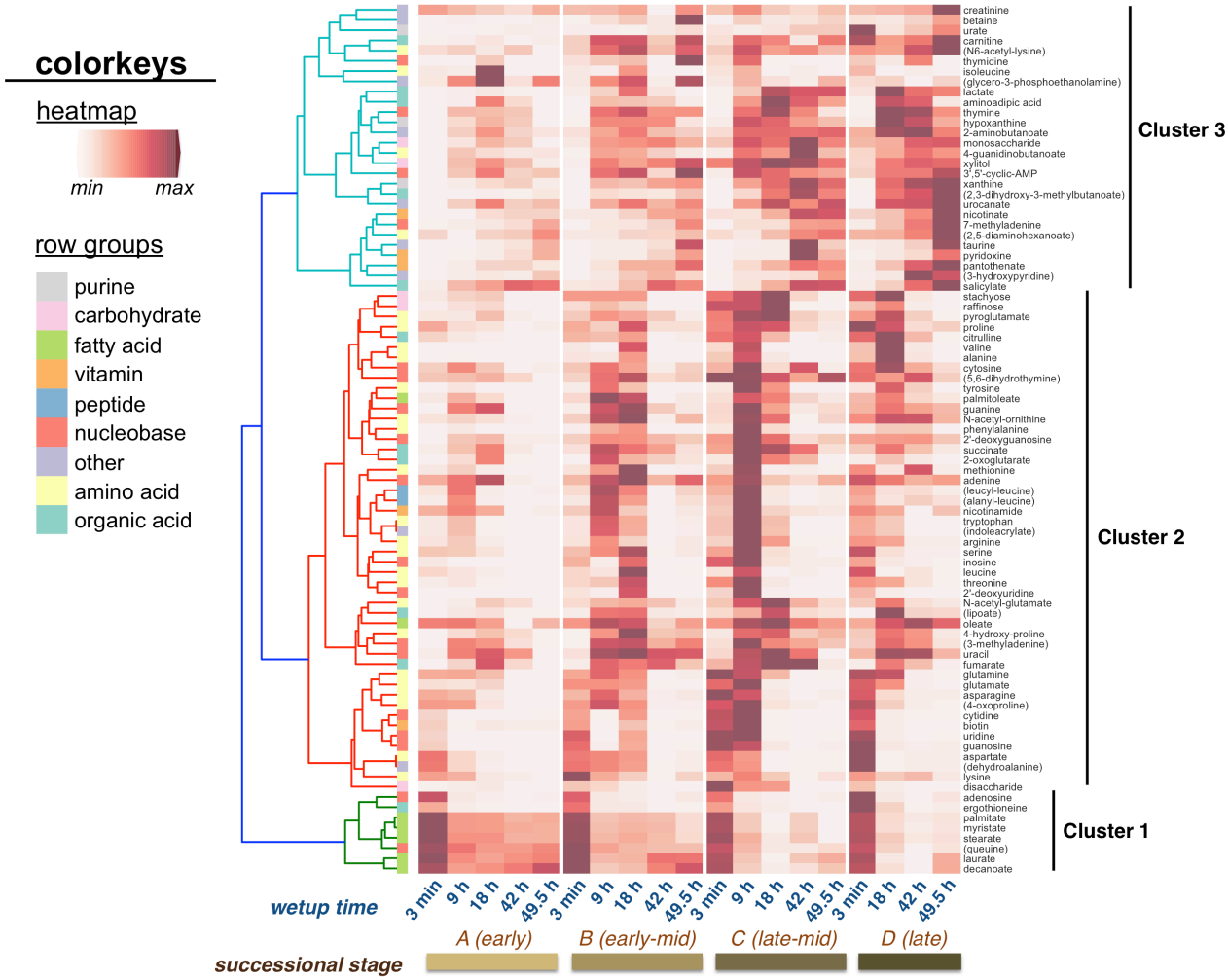


**Figure 2. Metabolite patterns detected in biocrust soil water.** Metabolite cycling, for a total of 85 metabolites, was observed in biocrust soil water across wetting and successional stages. Unique patterns are indicated by cluster 1 (early metabolites, fatty acids), cluster 2 (early- to mid-time point metabolites) and cluster 3 (late metabolites). Putative metabolites are indicated by parentheses.

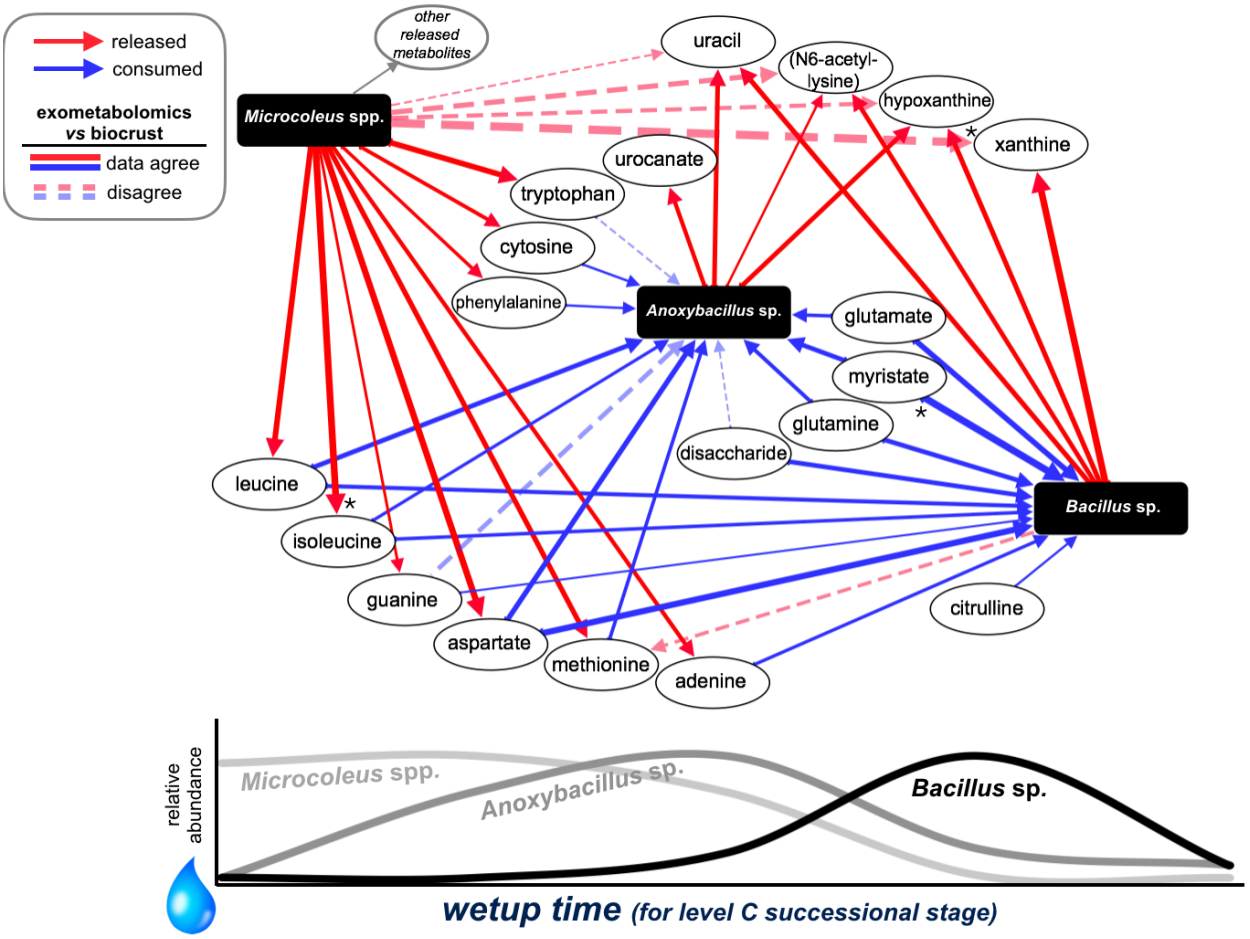


**Figure 3. Simplified biocrust foodweb of three dominant bacteria based on exometabolomic patterns.** This network displays the relationships between metabolites and three dominant organisms as they increase and decrease across wetting and successional stages in biocrust. As *Microcoleus* spp. immediately increases in relative abundance during early time points, many released metabolites (based on exometabolomics) are positively correlated with *Microcoleus* spp. (solid red arrows) and as the two relatively-abundant *Bacilli* increase (first *Anoxybacillus* sp. then *Bacillus* sp.), consumed metabolites decrease and are negatively correlated with these bacteria (solid blue arrows) and released metabolites are positively correlated (solid red arrows). Dotted arrows indicate metabolites that are released (red) or consumed (blue) that did not display the expected correlation relationship with that organism. The thickness of the line corresponds to the absolute value of the Spearman's *rho* correlation coefficient. * FDR < 0.05 for individual microbe-metabolite correlations. The expected directionality (solid lines versus dotted lines) was significant as determined by the exact binomial test ($p < 1 \times 10^{-5}$).

522

| Isolate ID from *Baran et al* (2015) | Related Biocrust Organism | Taxonomy | Percent Similarity[a] |
|---|---|---|---|
| *M. vaginatus* PCC9802 | *Microcoleus* spp. (*rplO* 1) | Cyanobacteria (p)/ Oscillatoriophycideae (c)/ Oscillatoriales (o)/ Microcoleus (f) | 92.0 |
| D1B51 | Anoxybacillus sp. (*rplO* 2) | Firmicutes (p)/ Bacilli (c)/ Bacillales (o)/ Bacillaceae (f)/ Anoxybacillus (g) | 86.3 |
| L2B47 | *Bacillus* sp. (*rplO* 60) | Firmicutes (p)/ Bacilli (c)/ Bacillales (o)/ Bacillaceae (f)/ Bacillus (g) | 87.6 |
| L1B44 | *Blastococcus* sp. (*rplO* 7) | Actinobacteria (p)/ Actinobacteria (c)/ Geodermatophilales (o)/ Geodermatophilaceae (f)/ Blastococcus (g) | 87.1 |

523 [a]Similarity in *rplO* sequence (isolate versus biocrust organism).

524

525 **Table 1.** Exometabolite-profiled isolates[20] and their closest phylotypes in biocrust**.**

526 **REFERENCES**


527 1. Paustian, K. *et al.* Climate-smart soils. *Nature* **532,** 49–57 (2016).
528 2. Friedlingstein, P. *et al.* Climate–carbon cycle feedback analysis: Results from the C4MIP
529 model intercomparison. *J. Climate* **19,** 3337–3353 (2006).
530 3. Judd, K. E., Crump, B. C. & Kling, G. W. Variation in dissolved organic matter controls
531 bacterial production and community composition. *Ecology* **87,** 2068–2079 (2006).
532 4. Collins, S. L. *et al.* A multiscale, hierarchical model of pulse dynamics in arid-land
533 ecosystems. *Annu. Rev. Ecol. Evol. Syst.* **45,** 397–419 (2014).
534 5. Siciliano, S. D. *et al.* Soil fertility is associated with fungal and bacterial richness, whereas
535 pH is associated with community composition in polar soil microbial communities. *Soil*
536 *Biol. Biochem.* **78,** 10–20 (2014).
537 6. Berthrong, S. T., Buckley, D. H. & Drinkwater, L. E. Agricultural management and labile
538 carbon additions affect soil microbial community structure and interact with carbon and
539 nitrogen cycling. *Microb. Ecol.* **66,** 158–170 (2013).
540 7. Maestre, F. T. *et al.* Increasing aridity reduces soil microbial diversity and abundance in
541 global drylands. *Proc Natl Acad Sci USA* **112,** 15684–15689 (2015).
542 8. Barnard, R. L., Osborne, C. A. & Firestone, M. K. Responses of soil bacterial and fungal
543 communities to extreme desiccation and rewetting. *ISME J* **7,** 2229–2241 (2013).
544 9. Placella, S. A., Brodie, E. L. & Firestone, M. K. Rainfall-induced carbon dioxide pulses
545 result from sequential resuscitation of phylogenetically clustered microbial groups. *Proc*
546 *Natl Acad Sci USA* **109,** 10931–10936 (2012).
547 10. Belnap, J., Weber, B. & Büdel, B. Biological Soil Crusts as an Organizing Principle in
548 Drylands. in *Biological Soil Crusts: An Organizing Principle in Drylands* (eds. Weber, B.,
549 Büdel, B. & Belnap, J.) 3–13 (Springer, 2016).
550 11. Maestre, F. T. *et al.* Structure and functioning of dryland ecosystems in a changing world.
551 *Annu. Rev. Ecol. Evol. Syst.* **47,** 215–237 (2016).
552 12. Elbert, W. *et al.* Contribution of cryptogamic covers to the global cycles of carbon and
553 nitrogen. *Nat. Geosci.* **5,** 459–462 (2012).
554 13. Garcia-Pichel, F. & Pringault, O. Cyanobacteria track water in desert soils. *Nature* **413,**
555 380–381 (2001).
556 14. Baldock, J. A. & Nelson, P. N. Soil Organic Matter. in *Handbook of Soil Science* (ed.
557 Sumner, M. E.) B25–B84 (CRC Press, 2000).
558 15. Schmidt, M. W. I. *et al.* Persistence of soil organic matter as an ecosystem property.
559 *Nature* **478,** 49–56 (2011).
560 16. Kogel-Knabner, I. The macromolecular organic composition of plant and microbial
561 residues as inputs to soil organic matter. *Soil Biol. Biochem.* **34,** 139–162 (2002).
562 17. Swenson, T. L., Jenkins, S., Bowen, B. P. & Northen, T. R. Untargeted soil metabolomics
563 methods for analysis of extractable organic matter. *Soil Biol. Biochem.* **80,** 189–198
564 (2015).
565 18. Warren, C. R. Comparison of methods for extraction of organic N monomers from soil
566 microbial biomass. *Soil Biol. Biochem.* **81,** 67–76 (2015).
567 19. Fierer, N. & Lennon, J. T. The generation and maintenance of diversity in microbial
568 communities. *Am. J. Bot.* **98,** 439–448 (2011).
569 20. Baran, R. *et al.* Exometabolite niche partitioning among sympatric soil bacteria. *Nat.*
570 *Commun.* **6,** 1–9 (2015).

21. Silva, L. P. & Northen, T. R. Exometabolomics and MSI: deconstructing how cells interact to transform their small molecule environment. *Curr. Opin. Biotechnol.* **34,** 209–216 (2015).
22. Yutin, N., Puigbo, P., Koonin, E. V. & Wolf, Y. I. Phylogenomics of prokaryotic ribosomal proteins. *PLoS ONE* **7,** (2012).
23. Hug, L. A. *et al.* A new view of the tree of life. *Nat. Microbiol.* **1,** 1–6 (2016).
24. Wu, M. & Eisen, J. A. A simple, fast, and accurate method of phylogenomic inference. *Genome Biol.* **9,** R151 (2008).
25. Sharon, I. *et al.* Accurate, multi-kb reads resolve complex populations and detect rare microorganisms. *Genome Res.* **25,** 534–543 (2015).
26. Garcia-Pichel, F. & Wojciechowski, M. F. The Evolution of a Capacity to Build Supra-Cellular Ropes Enabled Filamentous Cyanobacteria to Colonize Highly Erodible Substrates. *PLoS ONE* **4,** e7801–6 (2009).
27. Rajeev, L. *et al.* Dynamic cyanobacterial response to hydration and dehydration in a desert biological soil crust. *ISME J* **7,** 2178–2191 (2013).
28. Walsh, A. M. *et al.* Microbial succession and flavor production in the fermented dairy beverage kefir. *mSystems* **1,** e00052–16 (2016).
29. Ding, J. *et al.* Integrated metagenomics and network analysis of soil microbial community of the forest timberline. *Sci. Rep.* **5,** 7994–10 (2015).
30. Trivedi, P. *et al.* Microbial regulation of the soil carbon cycle: Evidence from gene-enzyme relationships. *ISME J* **10,** 2593–2604 (2016).
31. Garcia-Pichel, F., Lopez-Cortes, A. & Nubel, U. Phylogenetic and morphological diversity of cyanobacteria in soil desert crusts from the Colorado Plateau. *Appl. Environ. Microbiol.* **67,** 1902–1910 (2001).
32. Angel, R. & Conrad, R. Elucidating the microbial resuscitation cascade in biological soil crusts following a simulated rain event. *Environ. Microbiol.* **15,** 2799-2815 (2013).
33. Nicholson, W. L., Munakata, N., Horneck, G., Melosh, H. J. & Setlow, P. Resistance of Bacillus endospores to extreme terrestrial and extraterrestrial environments. *Microbiol Mol Biol Rev* **64,** 548–572 (2000).
34. Nicholson, W. L. Roles of *Bacillus* endospores in the environment. *Cell. Mol. Life Sci.* **59,** 410–416 (2002).
35. Pepe-Ranney, C. *et al.* Non-cyanobacterial diazotrophs mediate dinitrogen fixation in biological soil crusts during early crust formation. *ISME J* **10,** 287-298 (2016).
36. Hosoya, S., Lu, Z., Ozaki, Y., Takeuchi, M. & Sato, T. Cytological analysis of the mother cell death process during sporulation in bacillus subtilis. *J. Bacteriol.* **189,** 2561–2565 (2007).
37. Upton, A. C. & Nedwell, D. B. Nutritional flexibility of oligotrophic and copiotrophic antarctic bacteria with respect to organic substrates. *FEMS Microbiol Ecol* **62,** 1–6 (1989).
38. Garcia-Pichel, F., Loza, V., Marusenko, Y., Mateo, P. & Potrafka, R. M. Temperature drives the continental-scale distribution of key microbes in topsoil communities. *Science* **340,** 1574–1577 (2013).
39. Ferrenberg, S., Reed, S. C. & Belnap, J. Climate change and physical disturbance cause similar community shifts in biological soil crusts. *Proc Natl Acad Sci USA* **112,** 12116–12121 (2015).
40. Erbilgin, O. *et al.* Dynamic substrate preferences and predicted metabolic properties of a simple microbial consortium. *BMC Bioinformatics* accepted (2017).

41. Behrends, V., Ebbels, T. M. D., Williams, H. D. & Bundy, J. G. Time-resolved metabolic footprinting for nonlinear modeling of bacterial substrate utilization. *Appl. Environ. Microbiol.* **75,** 2453–2463 (2009).
42. Seth, E. C. & Taga, M. E. Nutrient cross-feeding in the microbial world. *Front Microbiol* **5,** 1–6 (2014).
43. Ponomarova, O. & Patil, K. R. Metabolic interactions in microbial communities: untangling the Gordian knot. *Curr. Opin. Microbiol.* **27,** 37–44 (2015).
44. Orsi, W. D. *et al.* Diverse, uncultivated bacteria and archaea underlying the cycling of dissolved protein in the ocean. *ISME J* **10,** 2158–2173 (2016).
45. Fike, D. A., Gammon, C. L., Ziebis, W. & Orphan, V. J. Micron-scale mapping of sulfur cycling across the oxycline of a cyanobacterial mat: a paired nanoSIMS and CARD-FISH approach. *ISME J* **2,** 749–759 (2008).
46. Woebken, D. *et al.* Revisiting $N_2$ fixation in Guerrero Negro intertidal microbial mats with a functional single-cell approach. *ISME J* **9,** 485–496 (2015).
47. Baran, R. *et al.* Metabolic footprinting of mutant libraries to map metabolite utilization to genotype. *ACS Chem. Biol.* **8,** 189–199 (2013).
48. Gougoulias, C., Clark, J. M. & Shaw, L. J. The role of soil microbes in the global carbon cycle: tracking the below-ground microbial processing of plant-derived carbon for manipulating carbon dynamics in agricultural systems. *J. Sci. Food Agric.* **94,** 2362–2371 (2014).
49. Stuart, R. K. *et al.* Cyanobacterial reuse of extracellular organic carbon in microbial mats. *ISME J* **10,** 1240–1251 (2016).
50. Malmstrom, R. R., Kiene, R. P., Cottrell, M. T. & Kirchman, D. L. Contribution of SAR11 bacteria to dissolved dimethylsulfoniopropionate and amino acid uptake in the North Atlantic Ocean. *Appl. Environ. Microbiol.* **70,** 4129–4135 (2004).
51. Kaiser, M. *et al.* The influence of mineral characteristics on organic matter content, composition, and stability of topsoils under long-term arable and forest land use. *J. Geophys. Res.* **117,** G02018 (2012).
52. Swenson, T. L., Bowen, B. P., Nico, P. S. & Northen, T. R. Competitive sorption of microbial metabolites on an iron oxide mineral. *Soil Biol. Biochem.* **90,** 34–41 (2015).
53. Lv, J. *et al.* Molecular-scale investigation with ESI-FT-ICR-MS on fractionation of dissolved organic matter induced by adsorption on iron oxyhydroxides. *Environ. Sci. Technol.* **50,** 2328–2336 (2016).
54. Martiny, J. B. H., Jones, S. E., Lennon, J. T. & Martiny, A. C. Microbiomes in light of traits: A phylogenetic perspective. *Science* **350,** aac9323–1 (2015).
55. Diamond, S., Jun, D., Rubin, B. E. & Golden, S. S. The circadian oscillator in *Synechococcus elongatus* controls metabolite partitioning during diurnal growth. *Proc Natl Acad Sci USA* **112,** E1916–E1925 (2015).
56. Orth, J. D., Thiele, I. & Palsson, B. Ø. What is flux balance analysis? *Nat. Biotechnol.* **28,** 245–248 (2010).
57. Allison, S. D. A trait-based approach for modelling microbial litter decomposition. *Ecol. Lett.* **15,** 1058–1070 (2012).
58. Zomorrodi, A. R. & Maranas, C. D. OptCom: A multi-level optimization framework for the metabolic modeling and analysis of microbial communities. *PLoS Comput. Biol.* **8,** e1002363 (2012).
59. Yao, Y. *et al.* Analysis of Metabolomics Datasets with High-Performance Computing and

Metabolite Atlases. *Metabolites* **5,** 431–442 (2015).

60. Smith, C. A. *et al.* METLIN: A metabolite mass spectral database. *Ther. Drug Monit.* **27,** 747–751 (2005).

61. Sumner, L. W. *et al.* Proposed minimum reporting standards for chemical analysis. *Metabolomics* **3,** 211–221 (2007).